EXPERIMENTAL STUDY ON FIVE-STORY FULL SIZE APARTMENT HOUSE OF REINFORCED CONCRETE WALLED FRAMES

Yorihiko Ohsaki*, Makoto Watabe** and Yutaka Matsushima***

Synopsis

This report is concerned with the experiment of 5-story full size apartment house of reinforced concrete walled frames, conducted by Building Research Institute entrusted by Japan Housing Corporation. The purpose of this experiment is to examine the characteristics of this type of structure under the seismic loading and to improve its structural design.

The special feature of this specimen lies in, in a word, its economic design which is considered to be close to the structural and working criteria - the thickness and the length of the wall are 15cm and 12cm/m^2 over the story, respectively, which are less than the limitations given by the requirements of Architectural Institute of Japan.

Tests are divided into two parts. One is the horizontal static loading test carried out until the specimen collapsed, and the other is the dynamic test to investigate vibration properties in both elastic and plastic zones.

The outline and results of these tests are presented together with the analyses of the test results.

1. Test Specimen

The plan and elevations of the test specimen as well as the whole set up of the various apparatus are shown in Figs. 1 - 4. Main properties of the building under experiment are as follows:

1. The building consists of five stories each of which has two apartments.
2. The area of each story is 13m x 7m = 91m^2 approximately.
3. The whole structure is of about 14m height above the floor level of the testing laboratory.
4. Total weight is about 420t, and 320t without the foundation.
5. The walls in both directions are of 15cm thickness. The length of the wall per unit area is 12.0cm/m^2 in the longitudinal direction, and 25.4cm/m^2 in the transverse one.
6. The horizontal design shearing force is 89.2t ≒ 90t on the first story, which corresponds to the load scale 1.
7. The mean shearing stress in the wall column of the first story in the case of design load is near to 4.9kg/cm^2.

* Dr. Eng., Head of Structures Division, Building Research Institute.
** Dr. Eng., Chief Research Member of International Institute of Seismology and Earthquake Engineering.
*** Dr. Eng., Research Member of International Institute of Seismology and Earthquake Engineering.

2. Method of Loading

2.1. Horizontal Static Loading

The loading was performed by the following two methods:

1) Individual loading on each floor.

The static loads were acting on each floor by three uniformly pressed link jacks as shown in Fig. 5. Every floor was being loaded individually.

This kind of loading was being carried out at both the initial and final stage of the experiment. The main purpose of the loading under consideration was to obtain the flexibility matrices of the structure.

2) Uniformly distributed loading

The static loads were acting on every floor by three uniformly pressed link jacks. All floors were being loaded simultaneously, as shown in Fig. 6. Accordingly, the load scale 1 means that the force per one jack is equal to 6 tons.

This loading simulates the inertia forces of the structure under the earthquake motion, of course. The distribution of forces over the height during the earthquake is presumed to be such a trapezoid as the upper parts are rather greater than the lower. However, the uniform loading was adopted considering the simplification and the correspondence to the design load as well.

2.2. Dynamic Loading

Dynamic loads were produced by the dynamic exciter of Building Research Institute. This exciter was located on the center of the roof of the specimen, whose maximum capacity of power was 10 tons. The tests were carried out five times according to the stages of failure of the specimen.

3. Measurement

The objects of the measurement are as follows. (Ref. Fig. 1 - 4)

1) Static measurement

i) Measurement of strains in concrete and reinforcements by wire strain gauges.

ii) Measurement of slope angles by clinometers.
iii) Measurement of displacements by dial-gauges and scales.
iv) Observation of cracks and taking photographs.

2) Dynamic measurement

Measurement of displacements of each floor and exciting frequencies.

4. Properties of Materials

Properties of the reinforcement and concrete obtained by the tests of materials are as follows.

Young's modulus of the reinforcement

$$E_s = 2.09 \times 10^6 \text{ kg/cm}^2$$

Yielding point of the reinforcement

$$\sigma_{sy} = 3.29 \text{ t/cm}^2$$

Initial young's modulus of concrete

$$E_{ci} = 2.72 \times 10^5 \text{ kg/cm}^2$$

General young's modulus of concrete

$$E_c = 2.19 \times 10^5 \text{ kg/cm}^2$$

Strength of concrete

$$F_c = 230 \text{ kg/cm}^2$$

5. THE RESULTS OBTAINED FROM THE STATIC TESTS

The outline of results obtained from the static tests are as follows:

1) The maximum strength for the first positive loading was 4.3 in load scale, 3.9 for the first negative one, 3.2 for the second positive one, and 2.9 for the second negative one. The ultimate strength decreased for every repetition of loading.

2) The order of the remarkable shearing cracks that occurred in the walled columns of the first story were as follows: (ref. Figs. 8 - 10 as for the details about the state of cracks.)

i) in the short columns of C-frame at the stage of 2.3 in load scale,
ii) in the side columns of C-frame at about 2.7,
iii) in the center columns of B-frame at about 3.0,
iv) in the side columns of B-frame and all columns of A-frame at the maximum load scale 4.3, respectively.

3) The mean shearing stress in columns at the stage when remarkable shearing cracks occurred in the short columns of C-frame at load scale 2.3 becomes about 11 kg/cm^2. This value corresponds to about 0.048 F_c.

4) The mean shearing stress in columns at the maximum load scale 4.3 becomes about 21 kg/cm^2, which almost corresponds to 0.091 F_c.

5) The relative horizontal displacement of the first story at the maximum loading was about 1.8 cm. This corresponds to about 1/140 in the rotation angle of the story.

6) The horizontal displacement of the top of the structure relative to the footing at the maximum loading was about 4.9 cm, which corresponds to about 0.98 cm in the mean story displacement.

7) The stiffness of C-frame is the greatest, and that of A-frame the smallest. The displacements of B-frame and C-frame as compared with that of A-frame were about 90% and 80% respectively. These ratios were almost constant regardless of the magnitude of loading.

8) The horizontal displacements over the height were distributed in so-called "shear-type" i.e., the story displacements of the lower stories were larger than the upper. The plastic deformation of the first story increased particularly when the load became greater, and the ratio between the deformation of the first story to the total one reached about 40%.

6. Static Analysis and Investigation

Referring to the above-mentioned test results, the static inelastic frame analysis are carried out with the following assumptions.

6.1. General assumptions in the analysis

1) The wall columns and girders are replaced into the straight line members considering the rigid zones and bending, shear deformation. The resultant frames are solved by the slope deflection method.

2) The length of the rigid zone and the effective width of the perpendicular member are taken as the same as given by the requirements of A.I.J.

3) The ultimate bending strength is calculated considering all of the reinforcements included in the effective section.

4) The ultimate shearing strength is calculated by the following equation, referring to the test results. This corresponds to 80% of the empirical formula given by Dr. Kokusho.

$$\tau_u = 0.11 F_c + 0.4 P_\omega \sigma_{sy}$$

in which τ_u : Ultimate shearing stress

F_c : Strength of concrete

P_ω : Web reinforcement ratio

σ_{sy} : Yielding strength of reinforcement

5) The slabs are assumed to be infinitely rigid, so the lateral displacement of each frame are uniform.

6) When the end of the member yields to the bending moment, the plastic zone, the length of which is 1/10 of the span, is assumed to be formed as shown in Fig. 11. The bending rigidity of this zone is assumed as 1/100

of that of the elastic one.

7) When the member is damaged by the shearing force, the equivalent plastic zones are supposed at both ends. The rigidity of these zones is taken as -1/1000 of that of the elastic one. (Ref. Fig. 12)

The negative sign of the plastic rigidity means the correspondence to the stress-strain relationship in case of the shearing failure. However, it is quite difficult how to give the absolute value to it. Though the very conservative value is used here considering the stability of calculation, the greater value will be expected in the actual case.

8) The loads increase monotonously until the frames collapse. The plastic zones once formed are assumed to remain in that condition.

9) The frames are assumed antisymmetric, so half of the structure is analysed.

6.2. Analytical results

According to the analytical results based on the above mentioned assumptions, the comparison between the analytical and experimental results are made.

The horizontal displacements of the top of the structure are shown in Fig. 13. The full line with black points and the other line represent the calculated and experimental results, respectively. There is a comparatively good agreement between them. Black points mean the steps on which the plasticity are developed. The numbers beside them represent the order of those steps.

The displacements of the first story are shown in Fig. 14 in the same manner as the previous figure. The calculated result is close to the experimental one, on the whole. Three lines located on the lower part represent the analytical distributed shearing force of A, B and C frame, respectively.

The negative rigidity in the shearing failure is taken as the very conservative value as mentioned previously, so C-frame still possesses the sufficient strength after short columns in it are damaged by the shearing force. However, the actual distributed shearing force of C-frame at the final stage is considered to have been much less.

The similar comparison as for the slope angle of the second floor joint of the center column in B-frame is shown in Fig. 15.

Figs. 16 - 18 show the comparison between the analysed and design values obtained by approximate method with respect to the stress distribution in the wall columns at the load scale 1. D-method in consideration of rigid zones and bending, shear deformation was used in the design approximation. It is found that there are rather differences between them. Especially, the evaluation of the rigidity of the wall with small openings in C-frame is worth noting.

Numbers in parentheses represent the shearing forces of the wall columns on the first floor calculated from the results measured by rosette gauges. Besides, numbers surrounded by rectangles mean the concentration factors of the shearing force which are equal to the ratios of the analysed shearing forces to the average ones, distributed in proportion to the wall length. It is found that the shearing force of A-frame is comparatively little, and that the stress is concentrated on the walls with small openings in C-frame, on the other hand.

The failure pattern of frames at the final stage is shown in Fig. 19. It is worth while to note that this analytical result is similar to the experimental one, referring to the crack pattern and the failure mode by the experiment. Numbers in Fig. 19 represent the order of the bending or shearing failures of members.

6.3. Analysis of the modified frames

As found by the above-described results, C-frame has the largest rigidity of all and the great stress concentration as the result. Especially the short columns in C-frame are collapsed by the shearing force at earlier stage and reduce their resisting ability. This will be not desirable for the aseismic design as is recognized by the damage during Tokachi-oki earthquake for example. In this sense, the walls with small openings in C-frame are tried to be changed into those with larger openings as shown in Fig. 20, and the resultant modified frames are analysed in the same manner.

Fig. 21 corresponds to Fig. 14 in the previous section. The distributed shearing forces in each frame on the first floor are now rather uniformly distributed in each frame The shearing failure which was produced in the original C-frame at the early stage does not occur in this case. The modified frames must be more ductile. This fact will be more clear by the comparison of the Fig. 22 to Fig. 19 which illustrate the failure pattern.

7. Results from the Dynamic Tests

7.1. Outline of the results

The fundamental natural periods and damping ratios obtained from five various dynamic tests are tabulated in Table 1 where M listed on the right hand side column represents the eccentricity moment of the generator.

The structure is considered to be almost elastic in D_1 and D_2 tests, to be developed into the plastic zones near to failure in D_3 test, and to be in the condition after the destruction in D_4 and D_5. The fundamental natural period increases about twice during D_1 through D_5. Moreover, when the eccentricity moment is taken to be greater in D_5, the natural period increases three times compared with the elastic case. Damping ratios are a little more than 2% in cases of the small amplitude.

7.2. Correspondence to the static tests

Spring constants of the structure are calculated from the slope of the fittest straight line to the hysteresis curve obtained by S_2 and S_3 test by means of the least square method. (Ref. Fig. 23). The fundamental periods and normal modes using these spring constants are calculated, the results of which

are shown in Fig. 24.

As S_2 and S_3 test are regarded as to correspond to D_2 and D_3 test respectively, the comparisons between them are presented in this figure. It is due to the above-mentioned calculation method of spring constants, in other words, due to the small amplitude during the dynamic tests that the natural periods and mode shapes calculated from the static tests are somewhat different from those resulted from the dynamic test.

8. DYNAMIC ANALYSIS

This section is concerned with the response analysis of the structure against the severe earthquakes considering the effect of the ground, after estimating the dynamic properties of the structure referring to the test results.

8.1. Vibration system

Though the foundation of the tested specimen was almost fixed on the floor of the laboratory, actual buildings have the flexible foundations, the effect of which can not be neglected.

The simple method often adopted in the problem of the interaction between the superstructure and soil is to transform the effect of soil into the swaying and rocking springs. This method is used herein for simplification, while the rocking motion is neglected because it may be considerably small in the longitudinal direction analysed.

Mass of the structure concentrated on each floor level is connected by the shear type springs. The final vibration system is shown in Fig. 25.

The values calculated from the static test S_3 are used for the spring constants of the superstructure. Mass at each floor level is determined after consideration of live loads, etc. that are assumed to be located on the actual structure. Spring constants of swaying K_h are given for three various soil conditions. Namely, horizontal soil coefficients K_h are assumed to be ∞, 2 and 1 kg/cm^3 corresponding to hard, medium and soft soils, respectively, from which spring constants K_h are determined. The fixed base conditions are assumed as the case of hard soil.

The fundamental normal modes of these systems are shown in Fig. 26, after normalization of the value of the top story to unity. The damping ratio concerning the fundamental vibration is given as 2.2% equally for all of these systems with the assumption of the internal viscous damping.

8.2. Strength and restoring force property

The initial ultimate strength of the superstructure is assumed to be 390 tons uniformly for every story in view of the result obtained from the static test. Restoring force properties of the structure are presented by the so-called shear failure model as shown in Fig. 27. This means that both stiffness and strength decrease for every yielding cycle. This type of hysteresis property will be suitable for the structure whose damage is caused by the shearing failure of columns.

The reduction factors of strength and stiffness are considered to be the function of number of yielding N and assumed to be expressed by the following equations.

The reduction factor of strength $\alpha = {}_a N$

The reduction factor of stiffness $\beta = {}_b N$

The constants a and b were determined from the experiment as:

$$a = 0.87, \qquad b = 0.65$$

The comparison between two equations above and the experimental results are shown in Fig. 28.

The strength of soil are assumed to be ∞ for hard soil, 390 tons which is equal to that of the superstructure for medium soil and its half-195 tons for soft soil. The restoring force characteristic of soil is taken as the elasto-plastic type as shown in Fig. 29. For the soil hysteresis properties, the values of α and β are always unity.

Vibration properties obtained from the above-mentioned procedure for three various systems are summarized on Table 2.

8.3. Ground motions

Ground motions adopted herein are the band limited white noises which will be considered to be almost equivalent to the actual severe earthquakes. Namely, the ground acceleration $\ddot{y}(t)$ is given by

$$\ddot{y}(t) = 15. \sum_{n=1}^{100} \cos\left\{2\pi(10t/n + \phi_n)\right\} \quad (\mathrm{cm/sec^2})$$

in which ϕ_n are the random number and $0 \leqslant \phi_n \leqslant 1$.

The duration t_d is taken as 10 second. This band limited white noise contains the waves with frequencies 0.1 - 10 c.p.s. uniformly, and its constant spectral density C_n, the root mean square $\sqrt{\ddot{y}^2}$ and the mean maximum acceleration $\ddot{y}_{max}$ are equal to the following values, respectively.

$$C_n = 15 \cdot t_d/2 = 75 \ \mathrm{cm/sec}$$

$$\sqrt{\ddot{y}^2} = \sqrt{(2/t_d^2) \cdot \sum_{n=1}^{100} C_n^2} \simeq 106 \ \mathrm{cm/sec^2}$$

$$\ddot{y}_{max} \simeq 335 \ \mathrm{cm/sec^2}$$

Five various band limited white noises with arbitrarily chosen phase angle ϕ_n were formed and utilized in the response calulation.

8.4. Results of the response

In Fig. 30 and 31 shown are the mean maximum absolute acceleration and story

shearing force respectively. The full, dotted and broken lines correspond to the hard, medium and soft soil, respectively.

In case of hard soil, the first story yields three or four times, but the others do not reach the ultimate strength. In case of medium soil, soil absorbs the vibration energy by yielding two or three times, and number of yielding in the first story are limited to one or two. In case of soft soil, soil yields as many as 23 or 4 times, and consumes most of energy. Every part in the superstructure remains below the ultimate strength.

In Fig. 32 and 33 shown are the mean maximum story displacement and ductility factor, respectively. The above-mentioned phenomena will be found more clearly.

8.5. Investigation

The results obtained from the inelastic response analysis with consideration of the ground effect are summarized as follows.

1) If the ground is considerably hard, this structure will suffer almost the same damage as that of the final stage of the static test during the severe earthquake.

2) If the structure stands on the standard soil, the damage by the severe earthquake will be almost equivalent to the situation after the static test S4.

3) If the soil is very soft and has capacity enough to absorb the energy, the damage will remain almost in the same condition as that after the static test S3.

9. Summary and Conclusions

The results from the static tests, dynamic tests and analyses are summarized as follows.

1) The structure with walled-frames whose dimensions are nearly close to the size of the relevant specimen, can be analysed by replacing these members into the equivalent straight line ones. However, only the elastic calculation is not sufficient for judgement. It is necessary to estimate the failure pattern of each member, especially of walled columns in order to judge the progress of failure precisely. It is intensely demanded to avoid such a member as is expected to cause shearing failure at the earlier stage.

2) It is an iron rule for the walled structure which resists the horizontal forces with its rigidity, that the rigidity and strength of each frame are given as uniformly as possible one another, and that wall should be arranged to avoid eccentricity.

3) It will be effective for the improvement of this structure as for 1) and 2) items that walls with small openings in C-frame are changed into those with large openings, for example.

4) This structure is considered to have almost the same damage during severe earthquakes as that of the final stage in the static test. Although, the above-mentioned degree of damages could be the maximum allowable limit, it must be noted that the execution of works should be carried out with the greatest possible care because thinness of the wall makes the works difficult and the defects in the execution will be apt to bring the unexpected big collapse.

10. Acknowledgements

This experiment was held by the members of "Housing Structure Committee" as shown in the following:

Housing Structure Committee

Chairman : Yorihiko Ohsaki, Head of the Structures Division.

Sub-Chairman : Yasuhiro Kameda, Head of the Production Division.

Members : 17 persons.

The authors want to express their thanks to whom it may concern for their helpful suggestions and assistance to this work.

TABLE 1

FUNDAMENTAL NATURAL PERIODS & DAMPING RATIOS

Symbols of dynamic tests	Fundamental natural period T_1 (sec.)	Fundamental damping ratio %	Eccentricity moment M (kgm)
D_1	0.149	2.24	2
D_2	0.152	2.59	2
D_3	0.170	2.22	2
D_4	0.290	-	2
D_5	0.435	3.26	20
	0.465	4.65	40
	0.485	3.40	60

TABLE 2

VIBRATION PROPERTIES

Story		Mass ($t \cdot cm^{-1} \cdot sec^2$)	Spring Constant ($t \cdot cm^{-1}$)	Ultimate strength (ton)	Yielding displacement (cm)
5		0.0733	423	390	0.922
4		0.0954	589	390	0.661
3		0.0954	636	390	0.614
2		0.0954	616	390	0.635
1		0.0954	564	390	0.690
F	Hard soil	0.239	∞	∞	-
	Medium soil		1400	390	0.279
	Soft soil		700	195	0.279

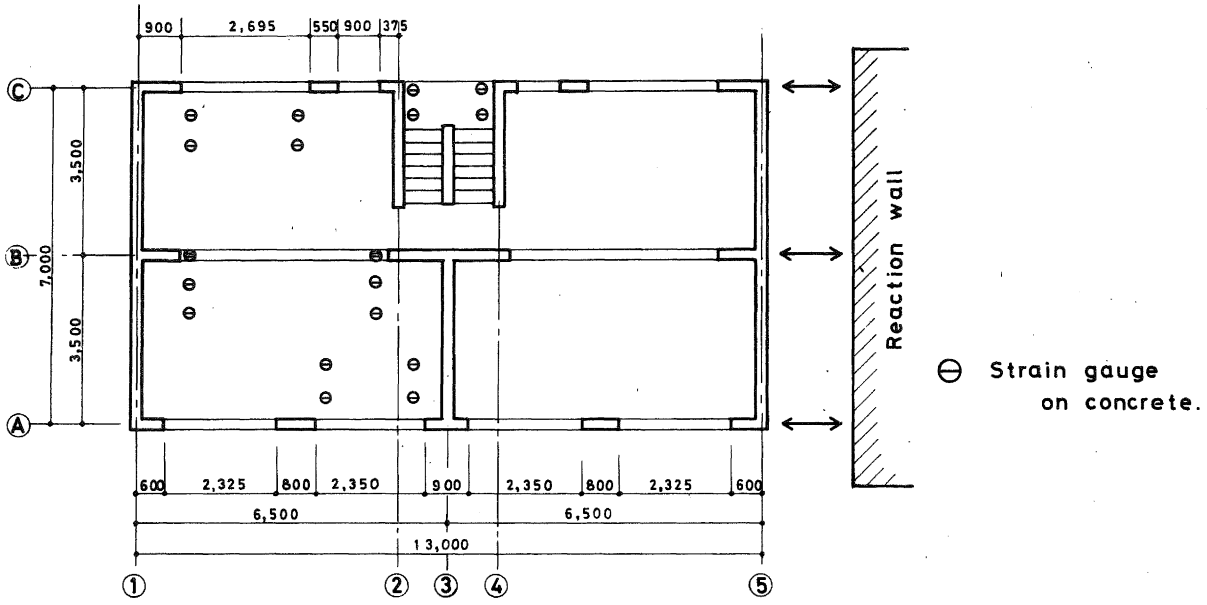

Fig. 1 Plan and positions of apparatus (2nd floor)

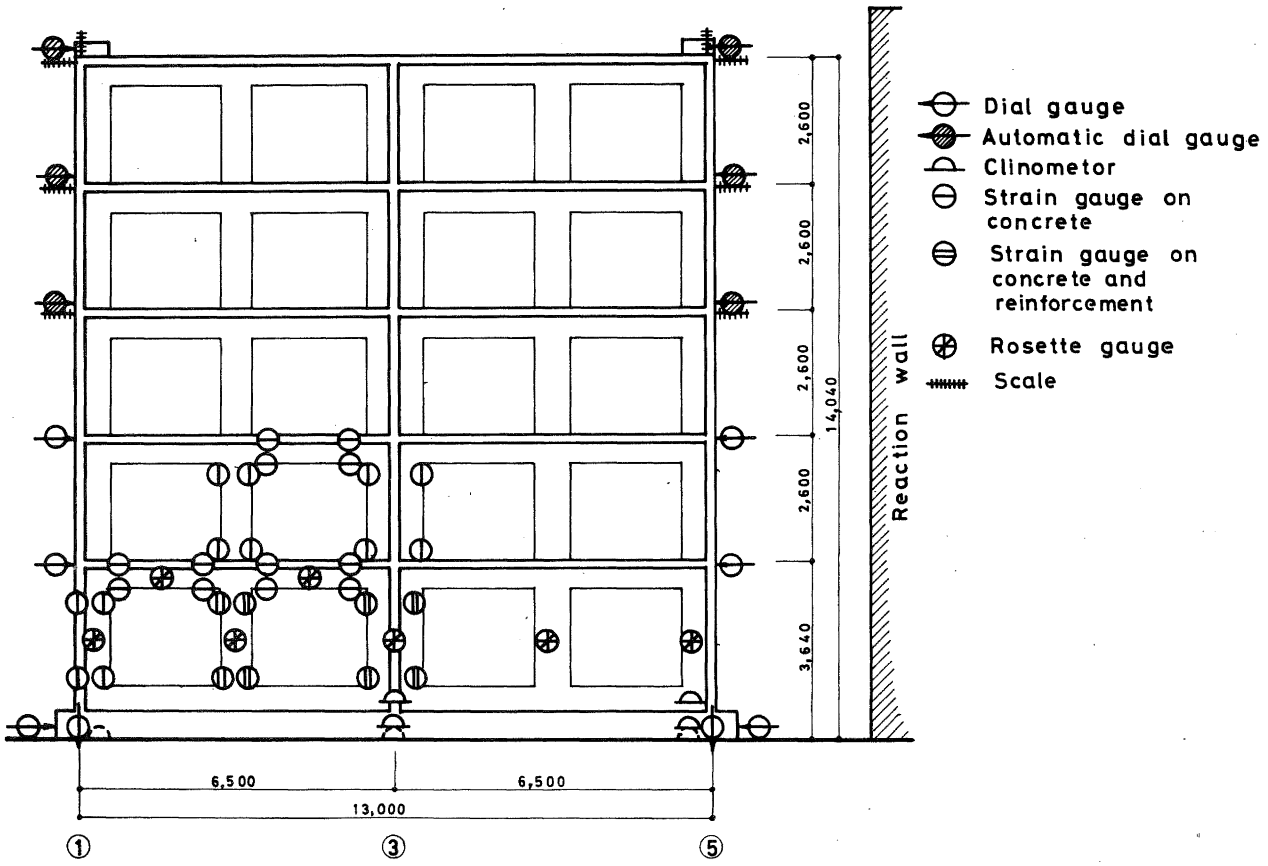

Fig. 2 Elevation and positions of apparatus (A-frame)

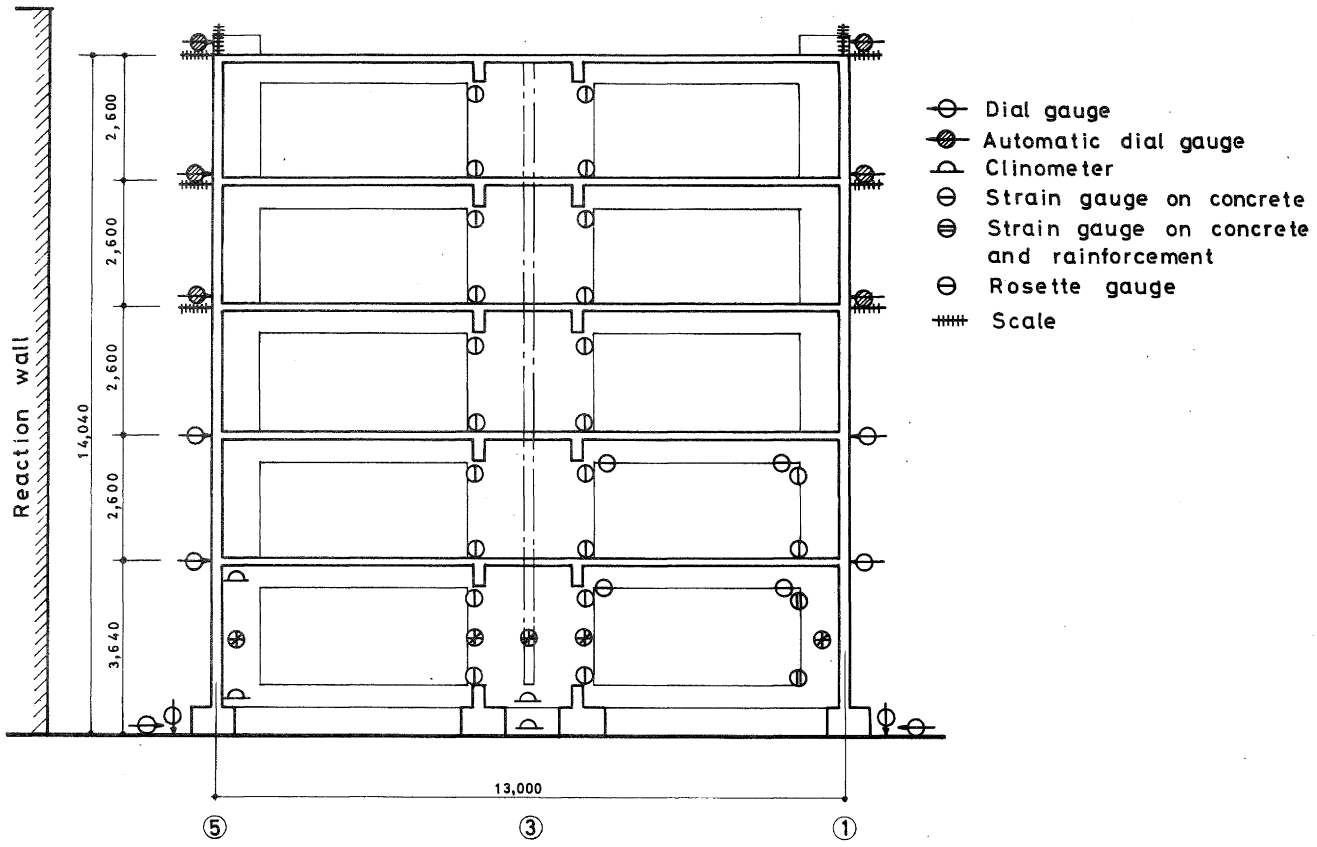

Fig. 3 Elevation and positions of apparatus (B-frame)

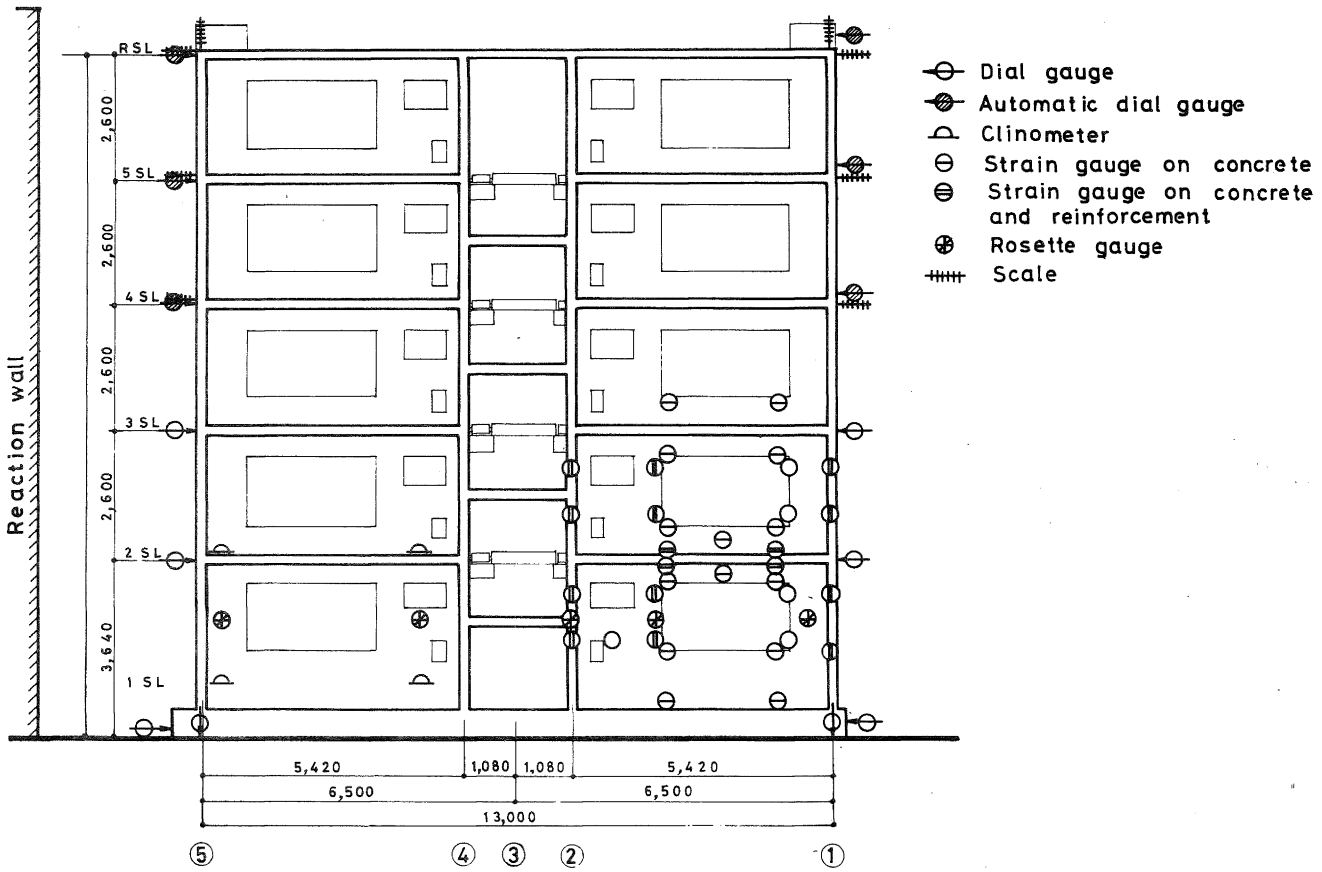

Fig. 4 Elevation and positions of apparatus (C-frame)

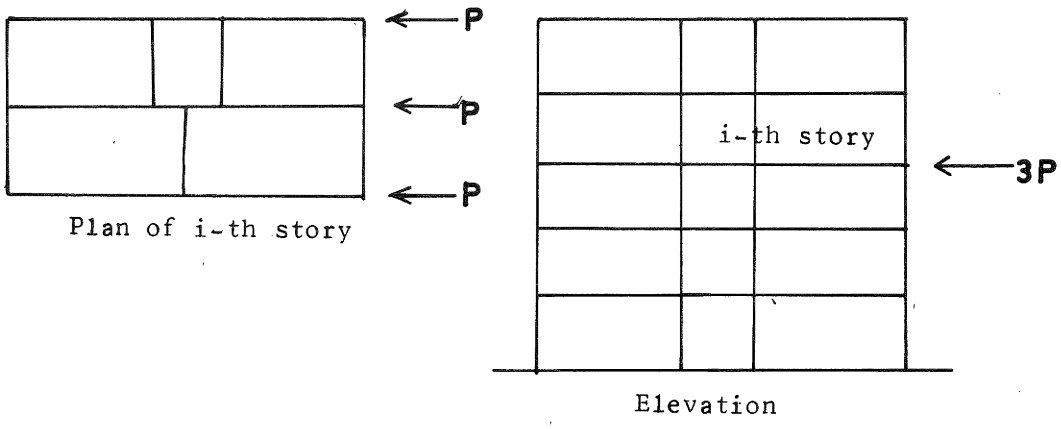

Fig. 5. Individual loading on each floor

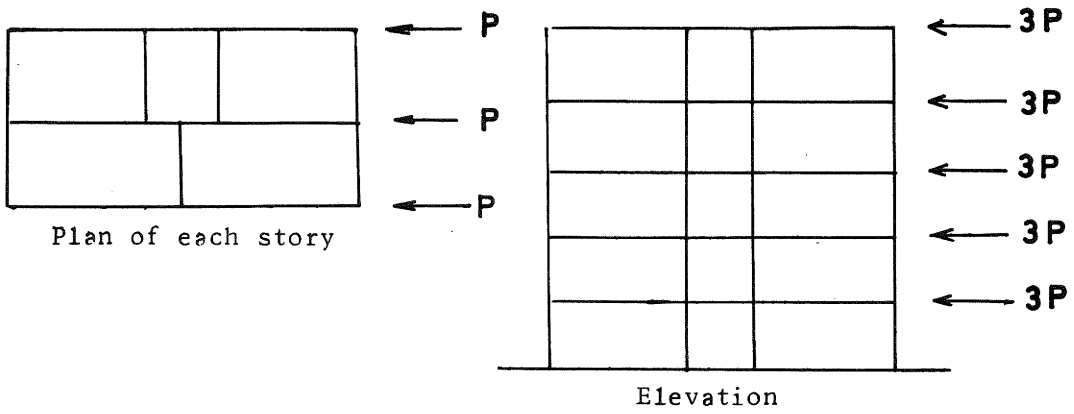

Fig. 6. Uniformly distributed loading

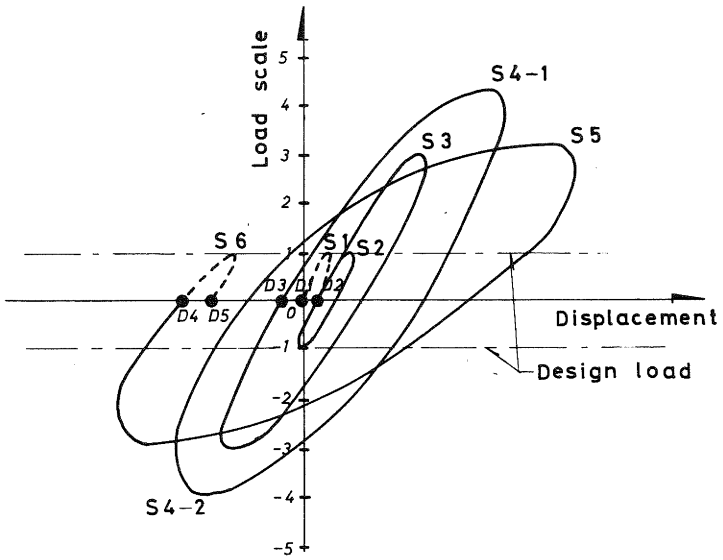

Fig. 7 Outline of various tests

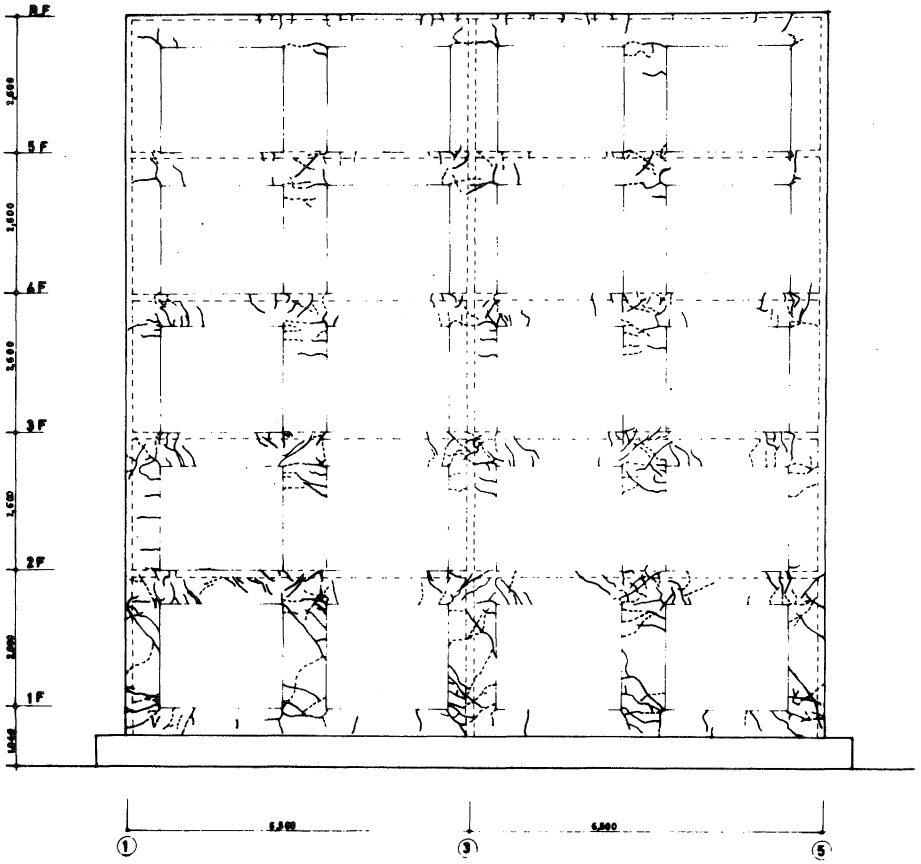

Fig. 8 State of cracks on A frame (At maximum load)

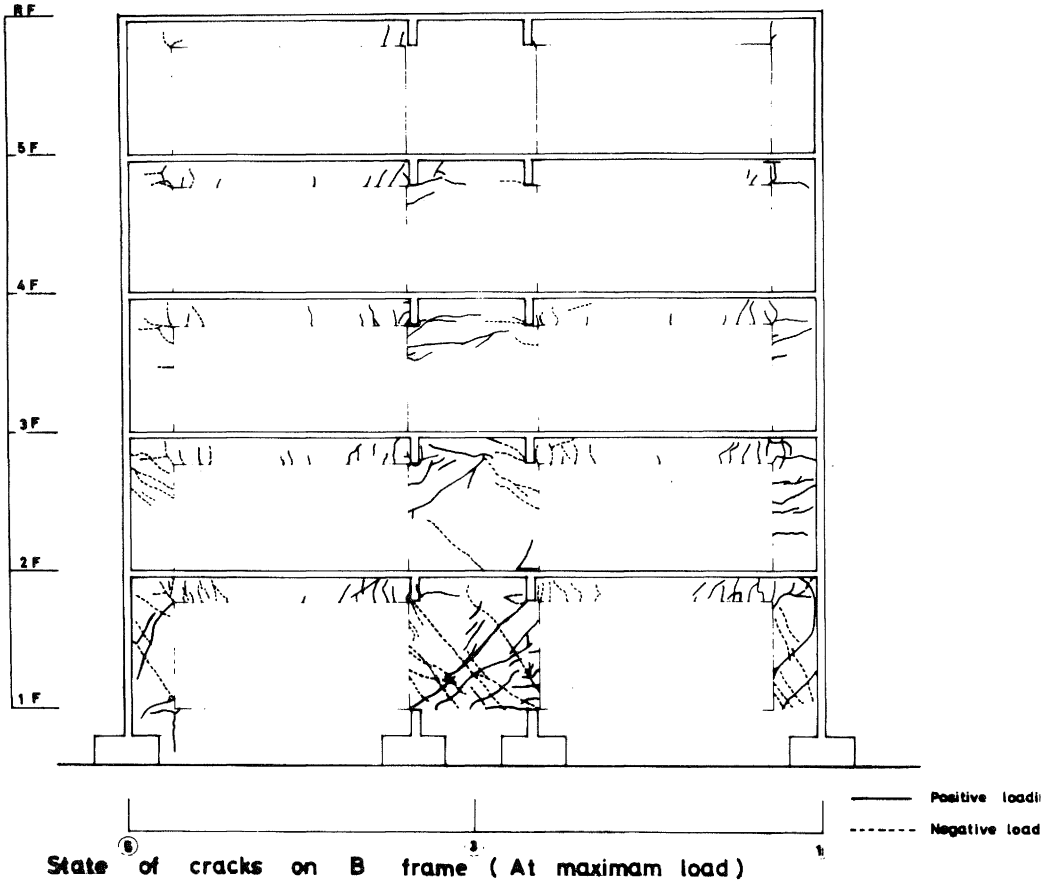

Fig. 9 State of cracks on B frame (At maximam load)

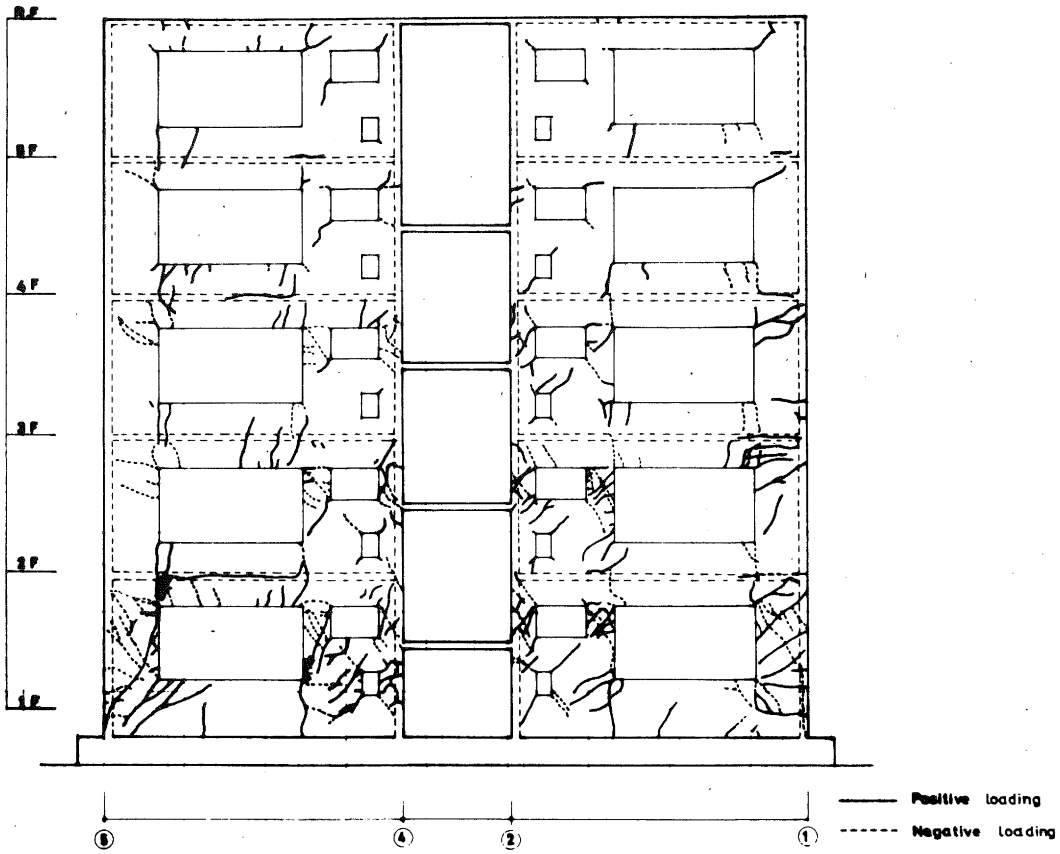

Fig. 10 State of cracks on C-frame (At maxmum load)

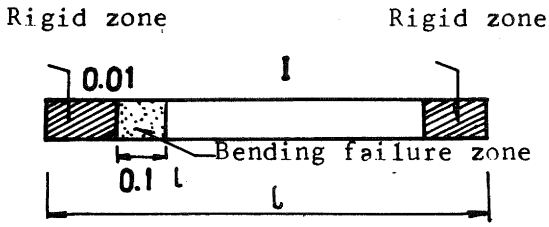

Fig. 11. Bending failure model

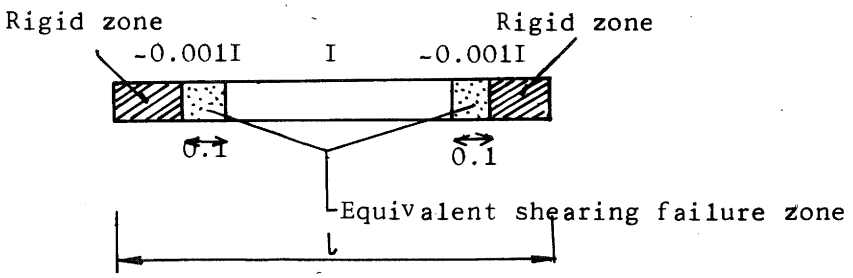

Fig. 12. Shearing failure model

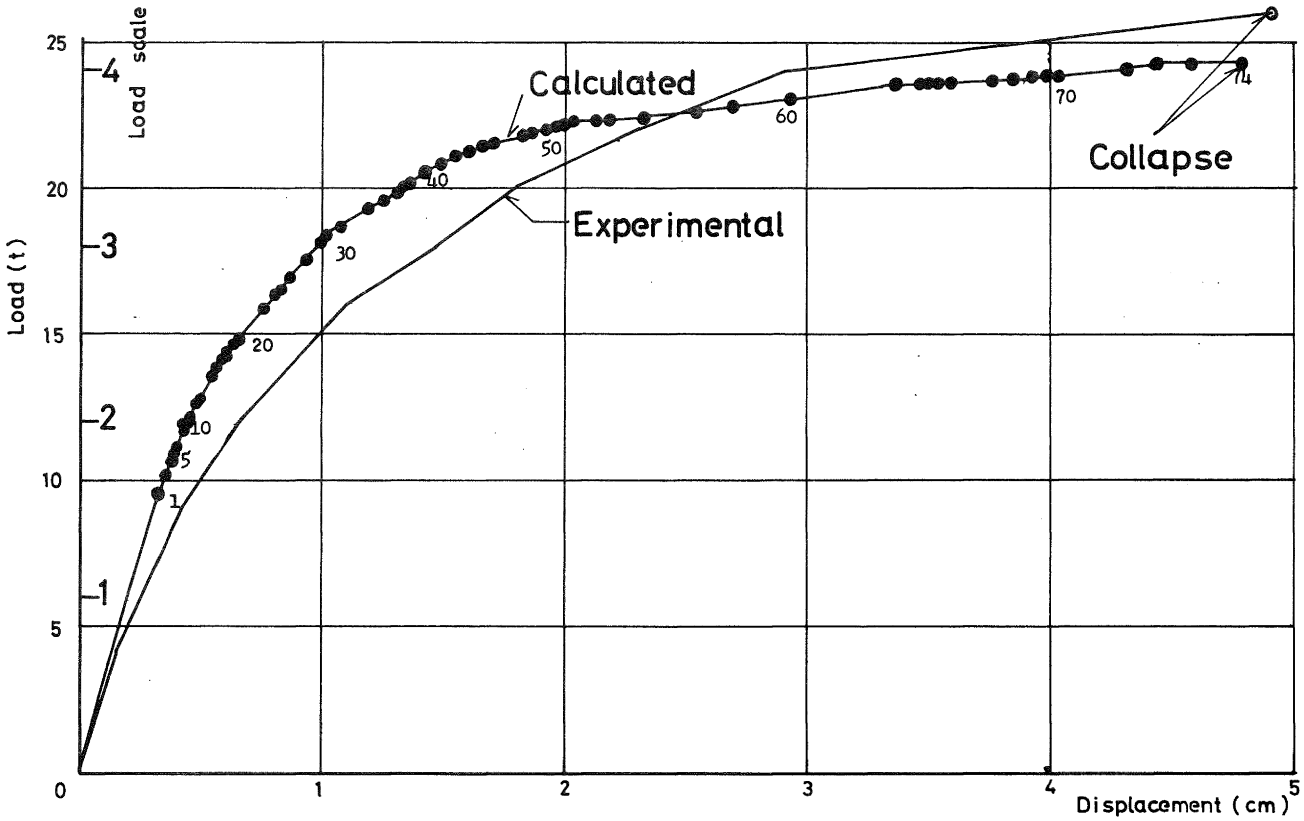

Fig. 13 Load-Displacement Curve of roof (Original frame)

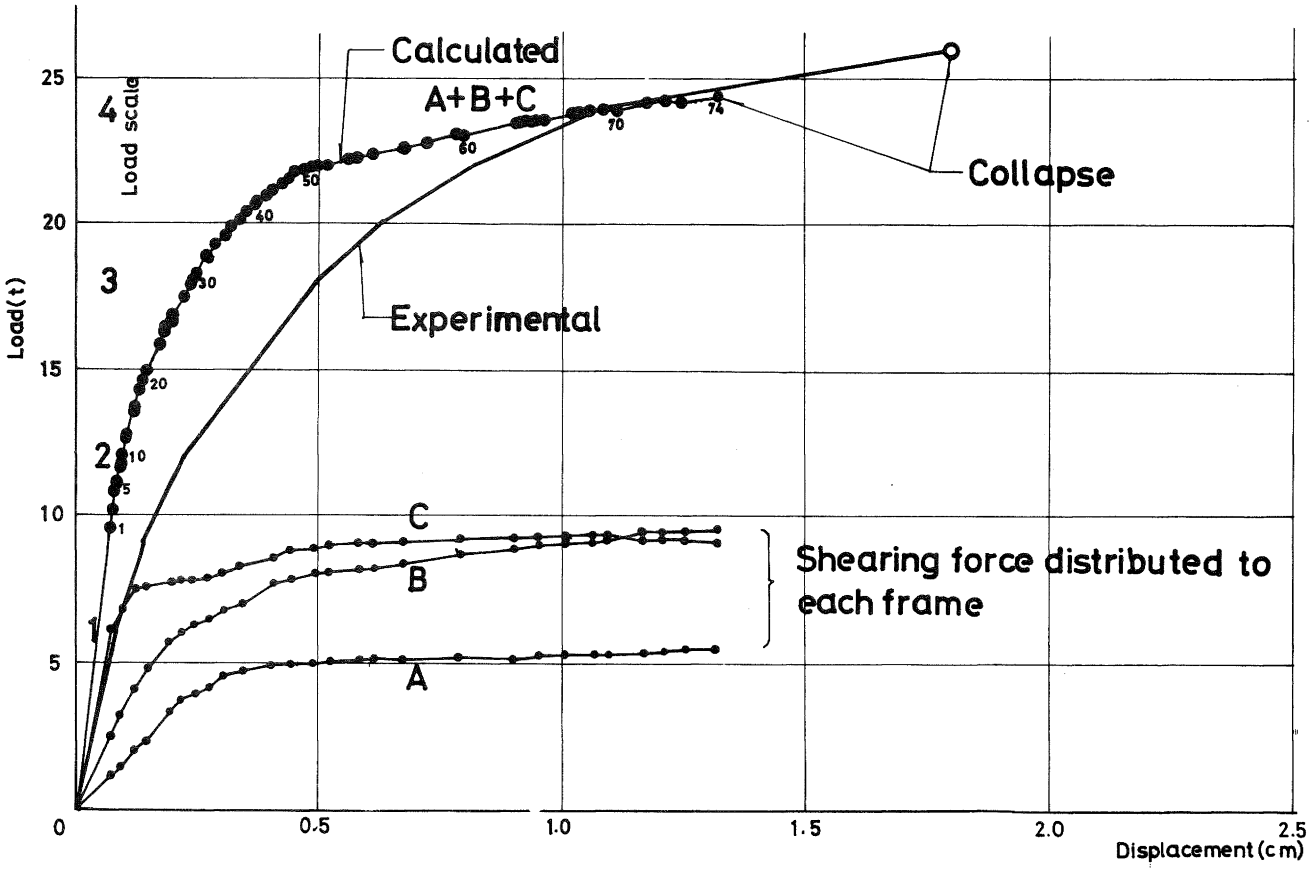

Fig. 14 Load-displacement curve of 2nd floor (Original frame)

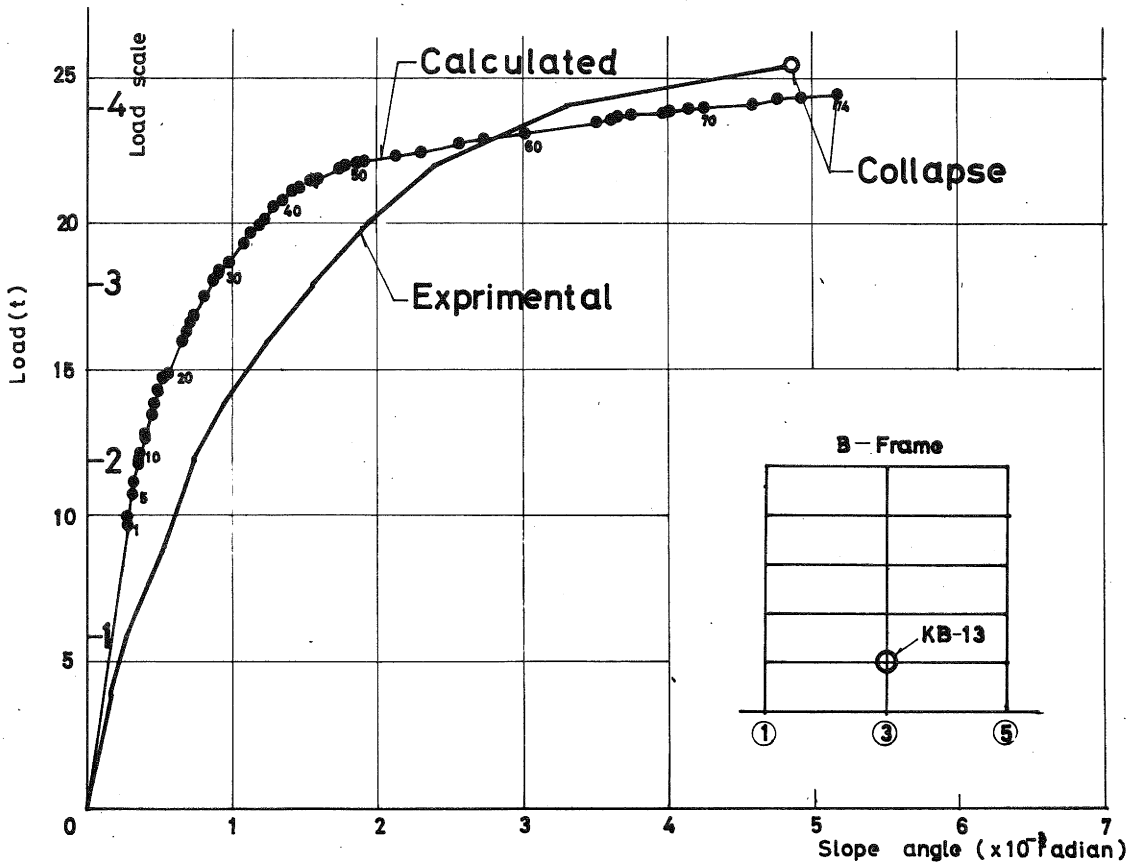

Fig. 15 Load-Slope angle curve (KB-13)

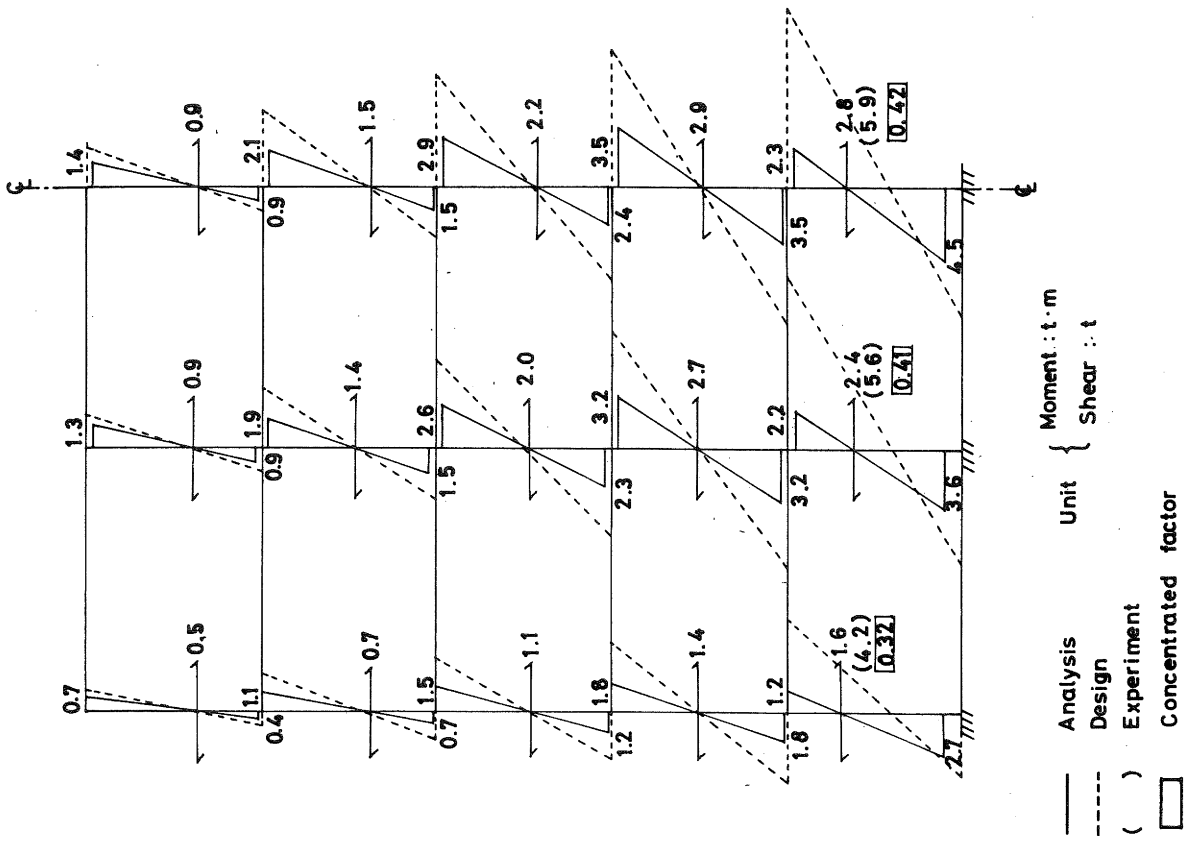

Fig.16 Stress distribution in walled columns of A-frame (At load scale 1)

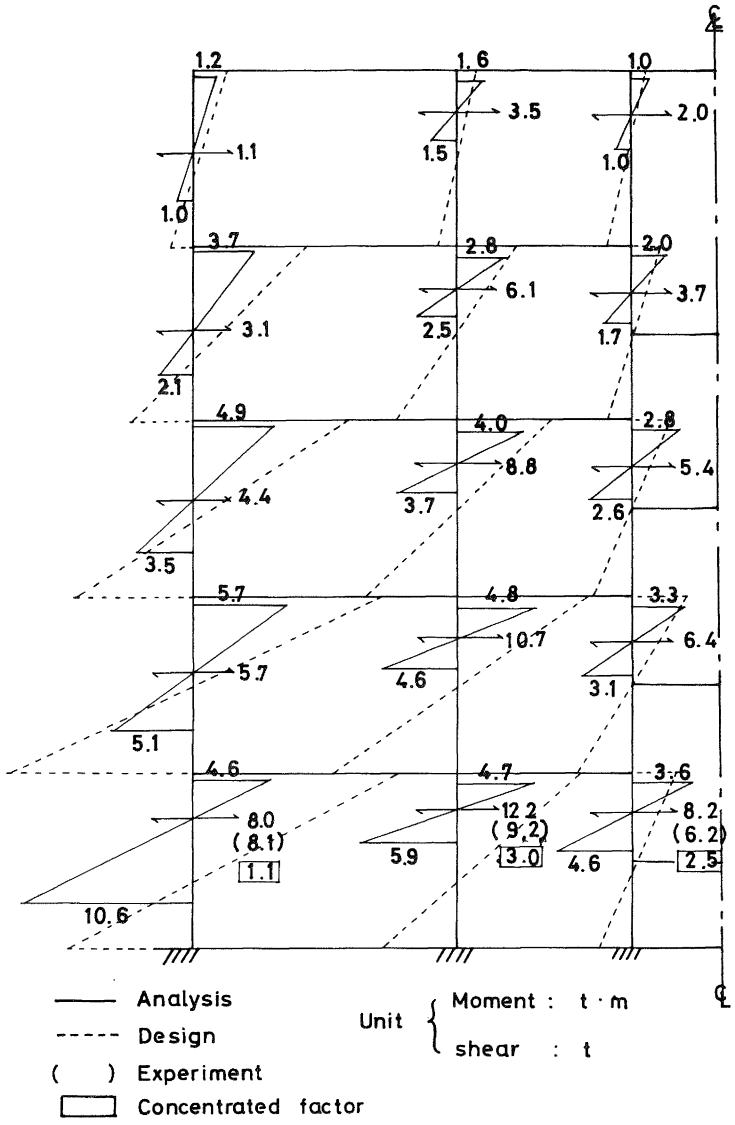

Fig.18 Stress distribution in walled columns of C frame (At load scale 1)

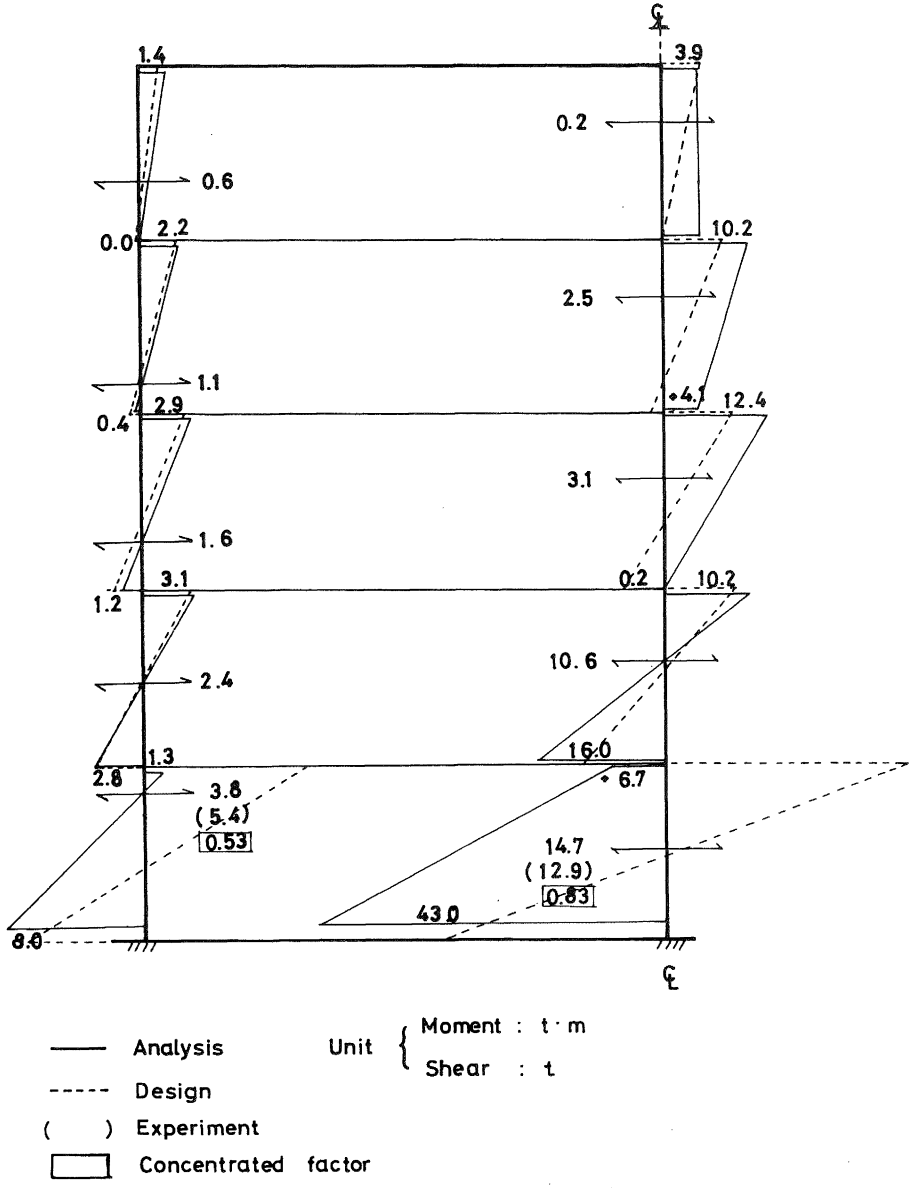

Fig.17 Stress distribution in walled columns of B frame (At load scale 1)

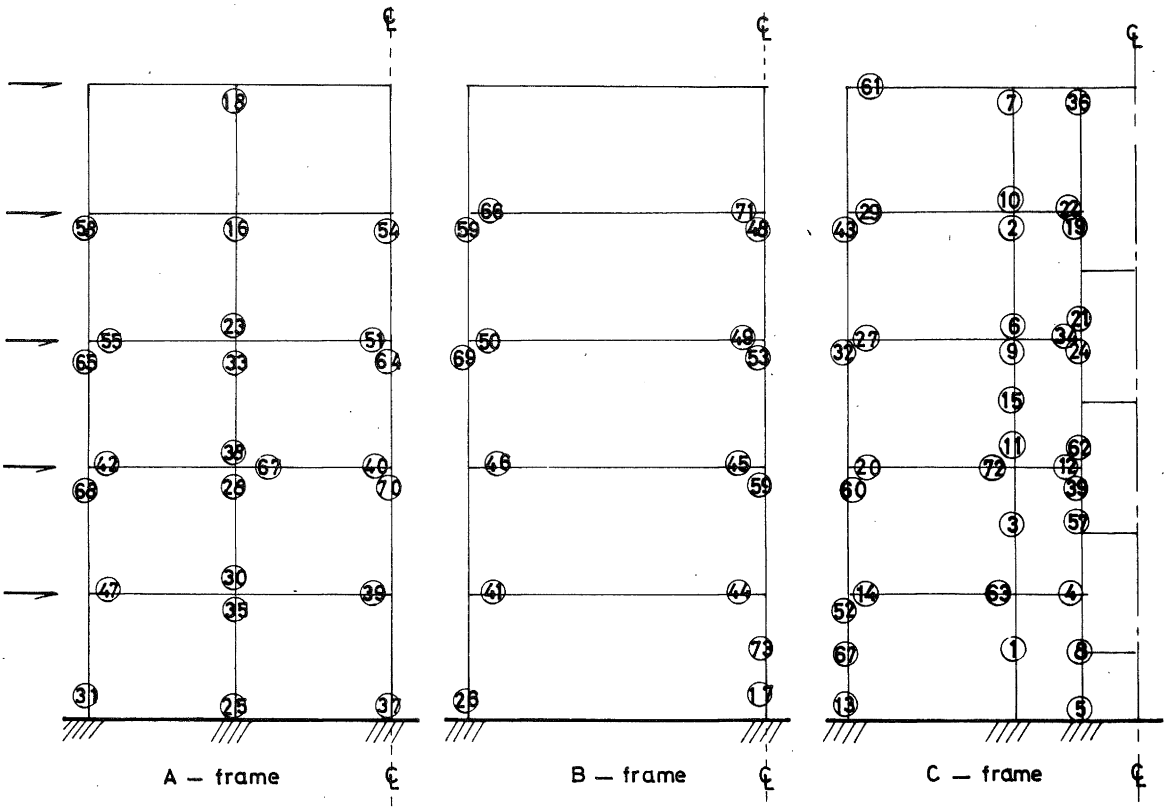

Fig. 19 Order of failures (Original frames)

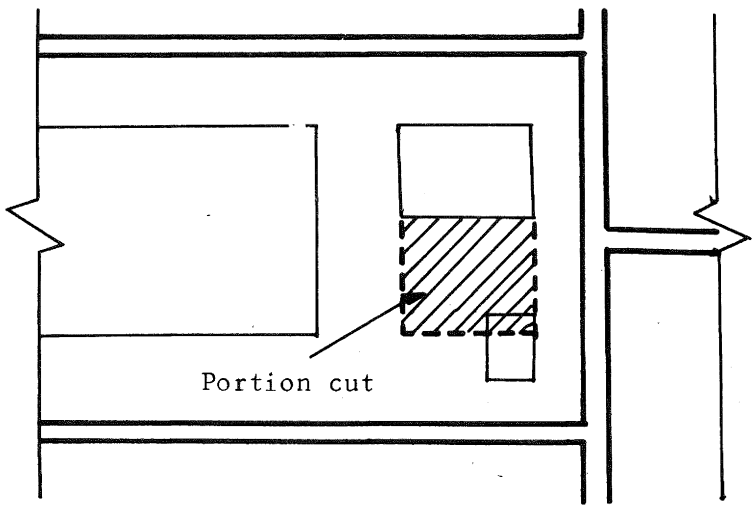

Fig. 20. Modified frame(Small openings of C-frame are enlarged.)

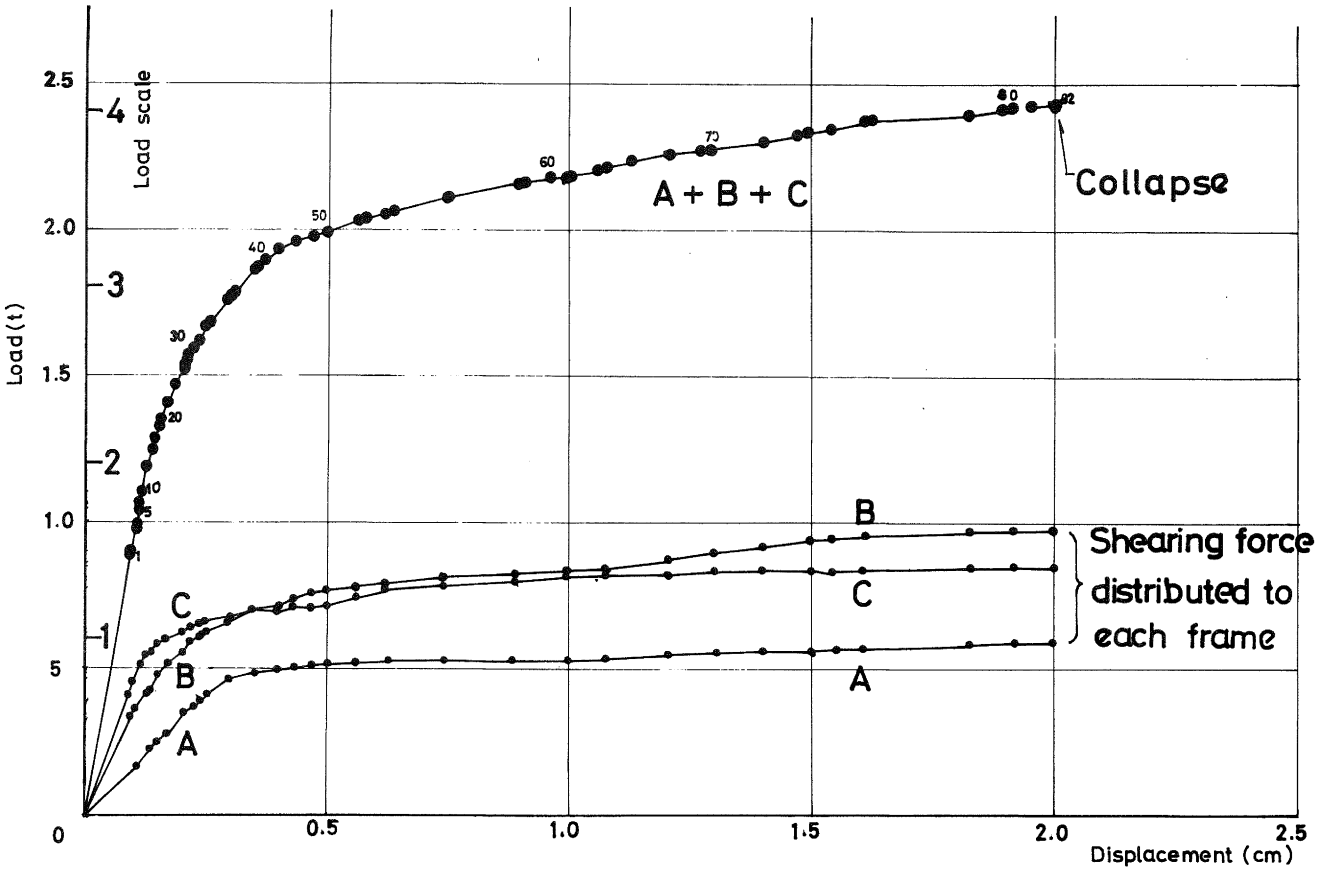

Fig. 21 Load displacement curve of 2nd floor (Modified frame)

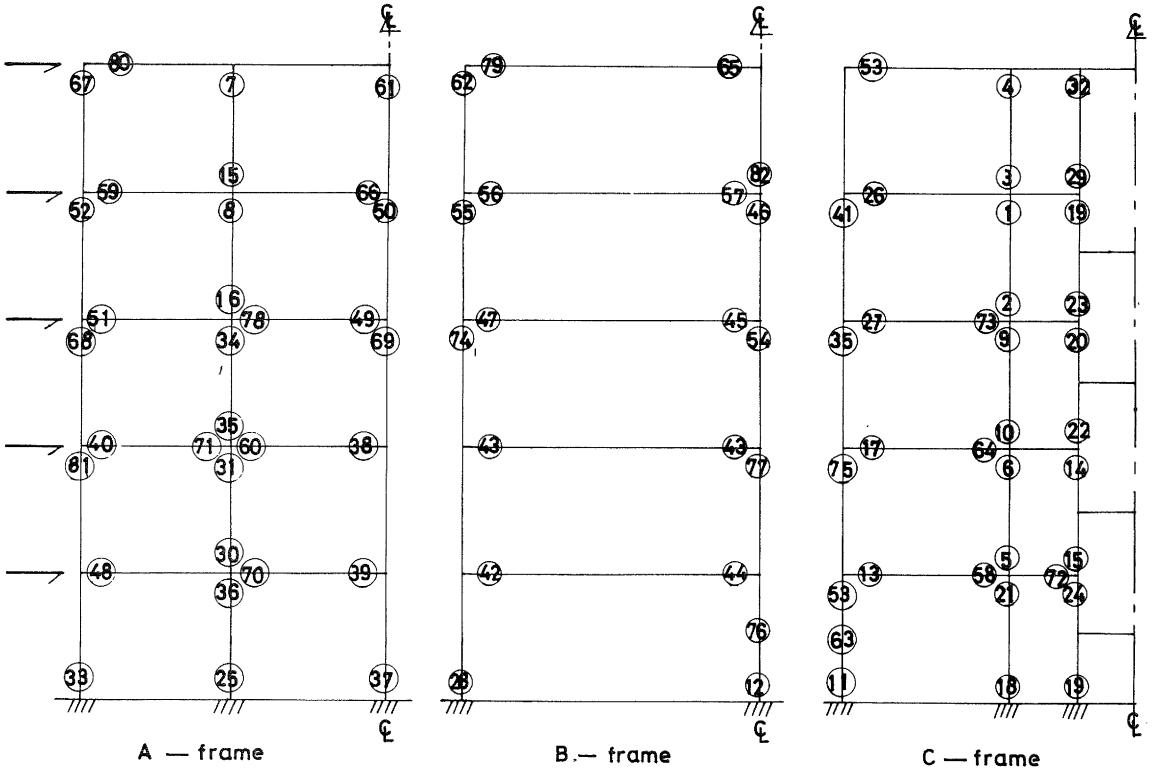

Fig. 22 Order of failures (Modified frames)

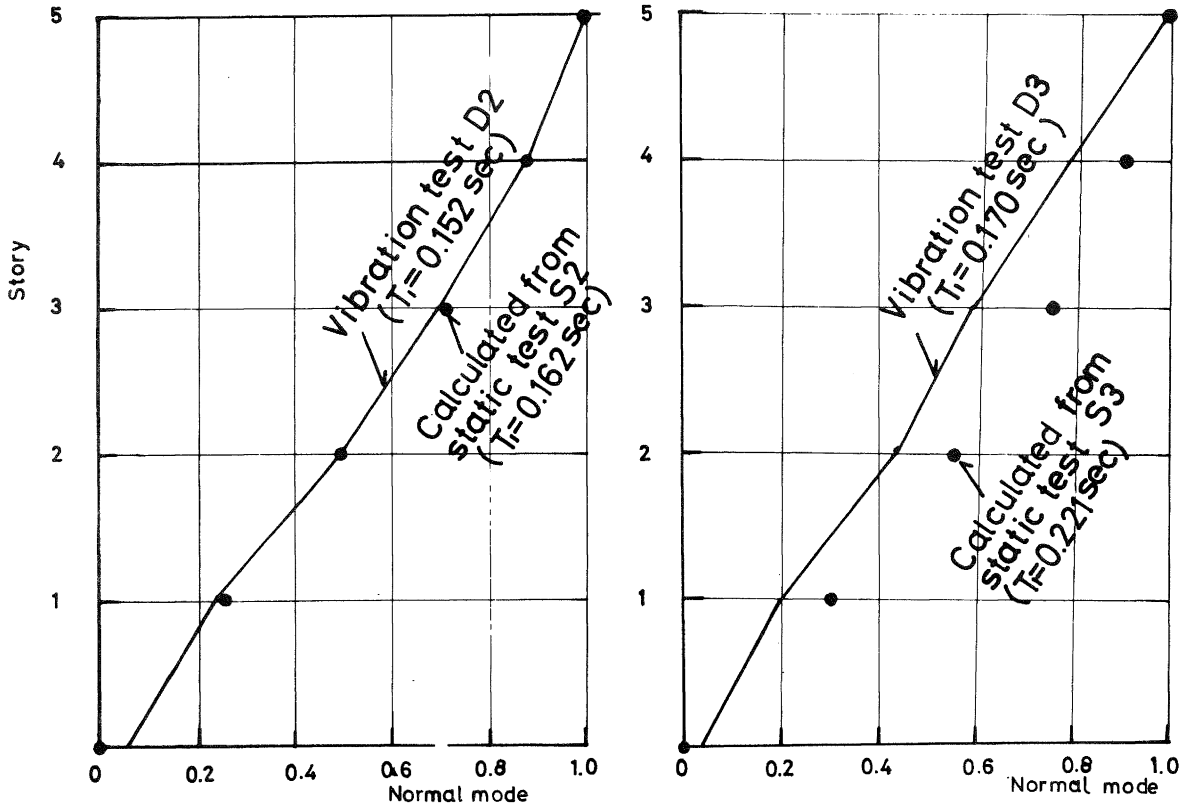

Fig. 24 Fundamental normal modes obtained by static and dynamic tests.

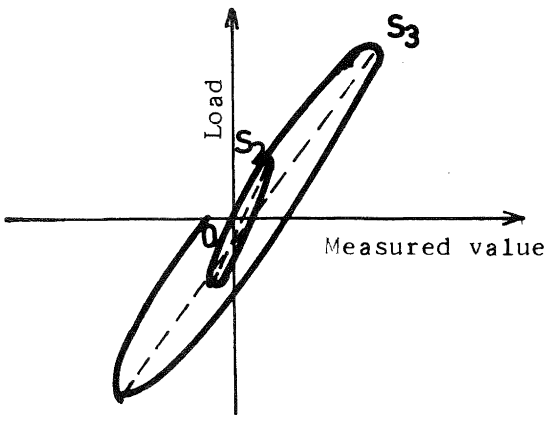

Fig. 23. Straight line approximation

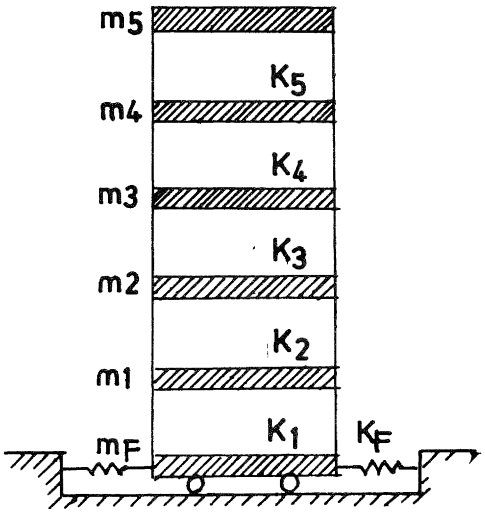

Fig. 25. Model of structure

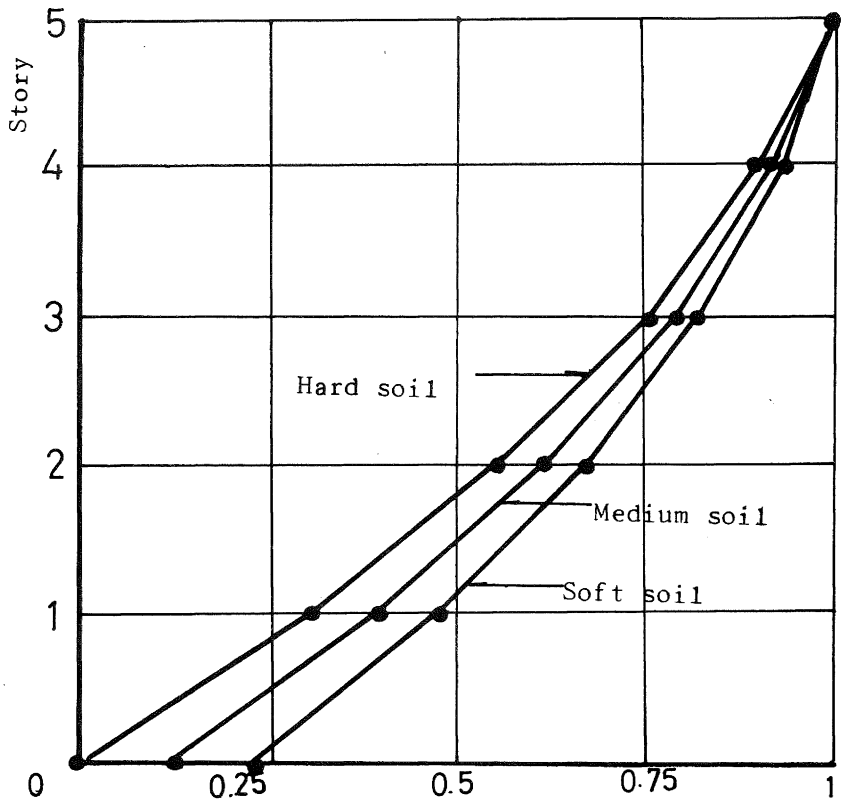

Fig. 26. Fundamental normal modes for 3 Various soil conditions.

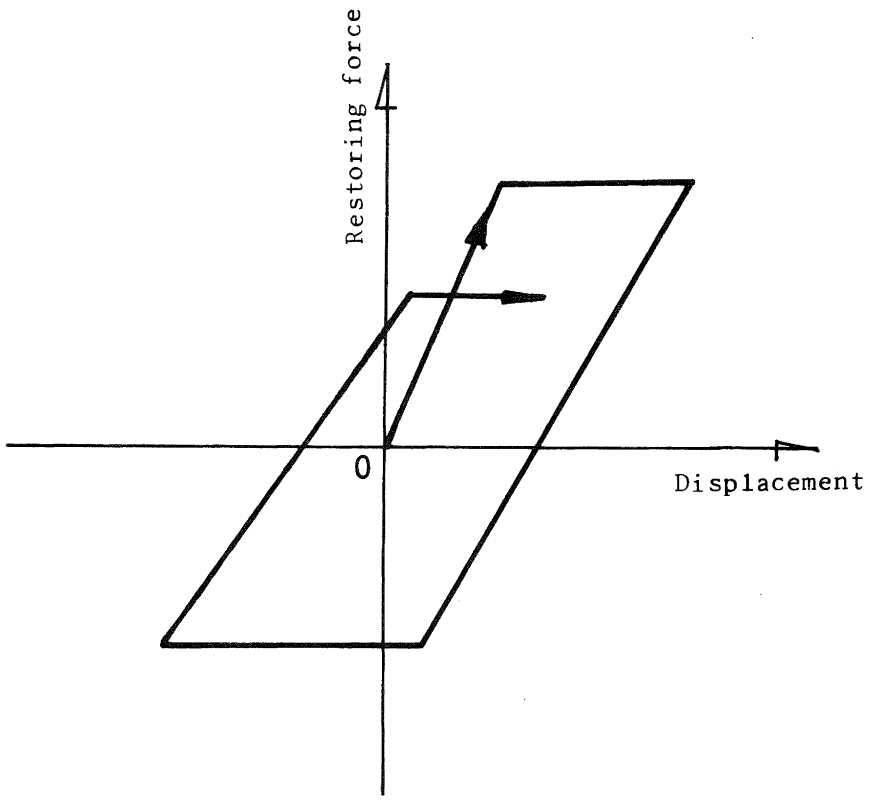

Fig. 27. Hysteresis curve for shearing failure type

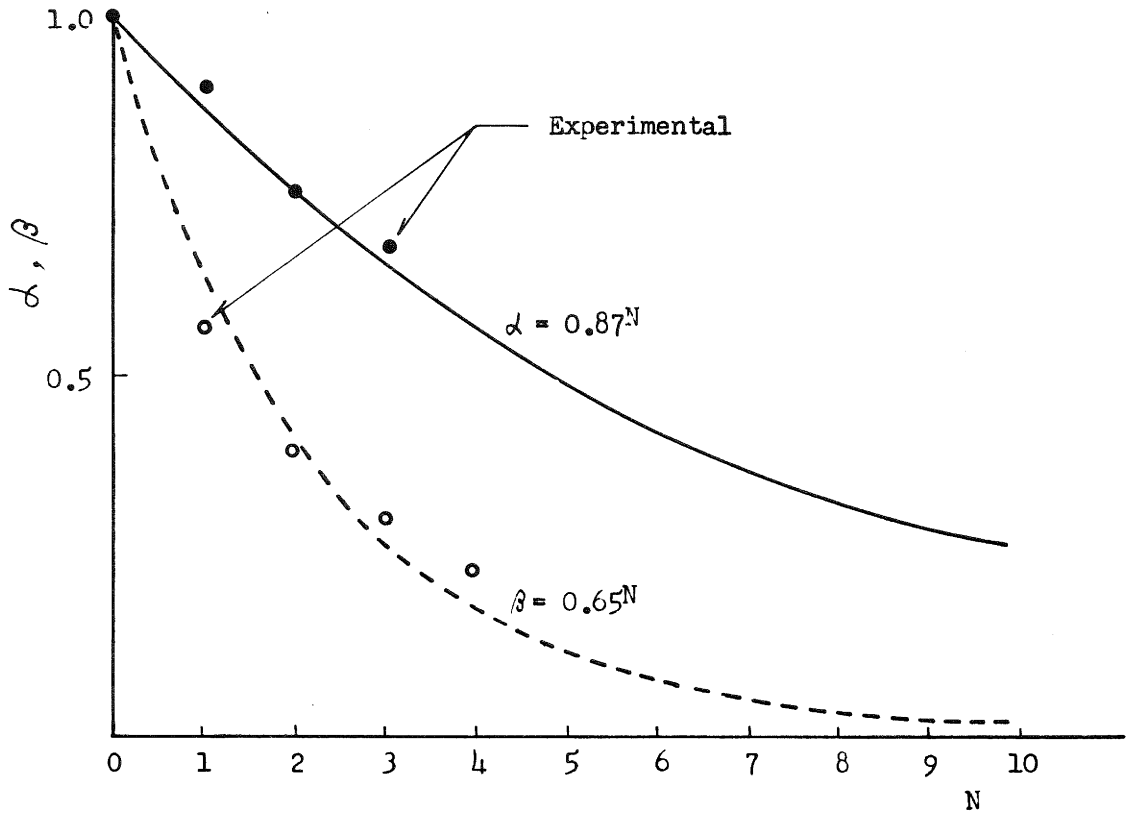

Fig. 28 Relation between strength or stiffness reduction factor and yielding number.

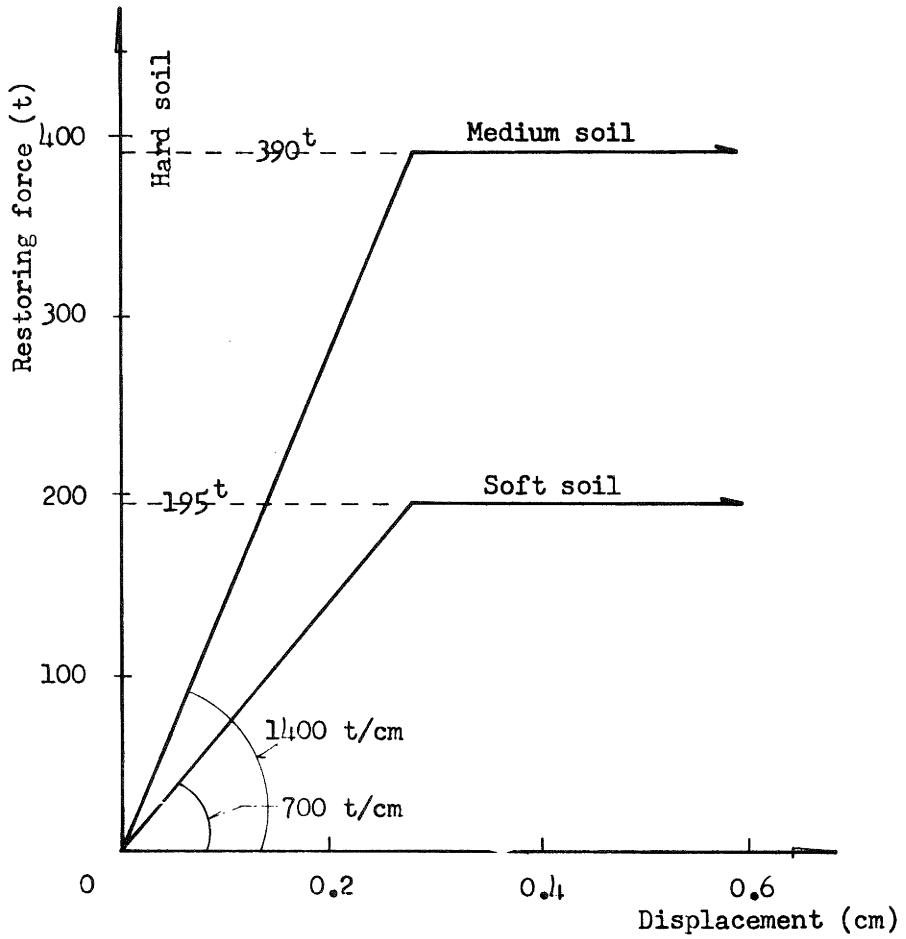

Fig. 29 Restoring force characteristics of soils

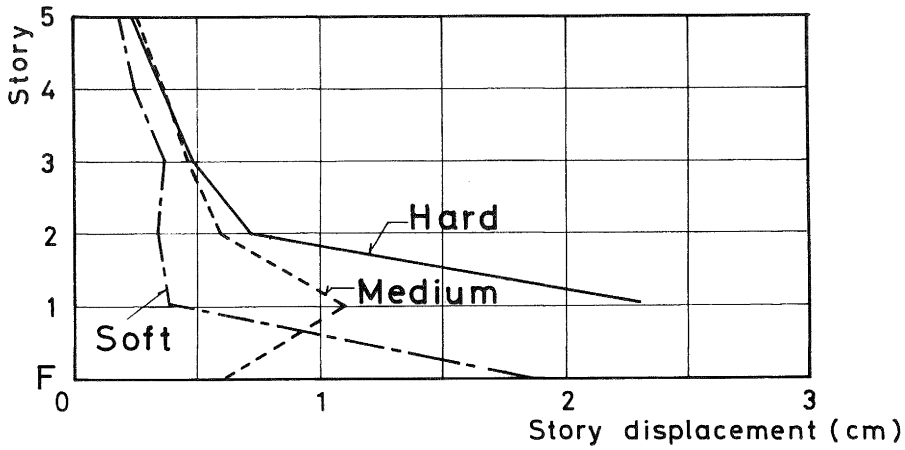

Fig. 32 Mean maximum story displacement

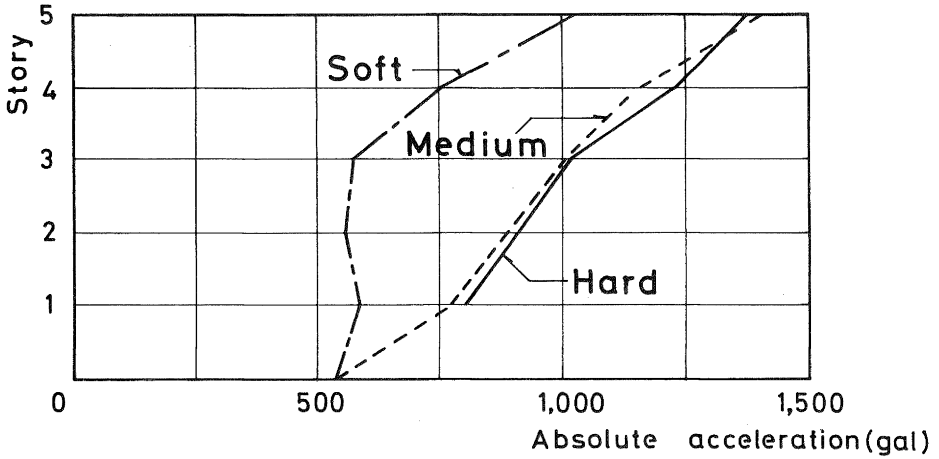

Fig. 30 Mean maximum absolute acceleration

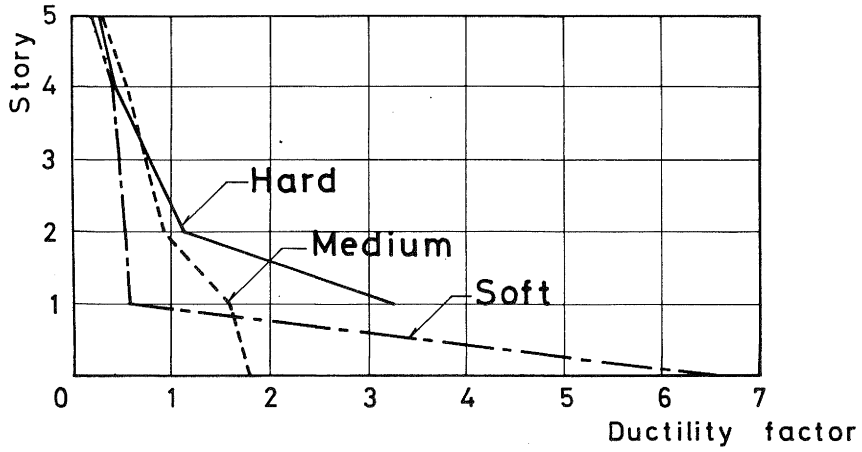

Fig. 33 Mean maximum ductility factor

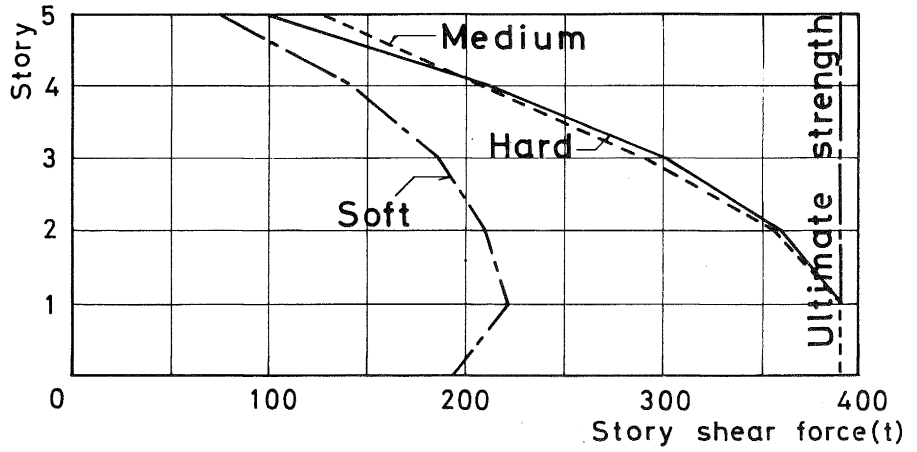

Fig. 31 Mean maximum story shear force